

It's all about the mirrors: Deep neural network assisted optimization of laser stabilization cavities

Johannes Dickmann (✉ j.dickmann@tu-braunschweig.de)

Technische Universität Braunschweig

Liam Shelling Neto

Technische Universität Braunschweig

Mika Gaedtke

Technische Universität Braunschweig

Stefanie Kroker

Technische Universität Braunschweig

Article

Keywords:

Posted Date: July 1st, 2022

DOI: <https://doi.org/10.21203/rs.3.rs-1776552/v1>

License:  This work is licensed under a Creative Commons Attribution 4.0 International License.

[Read Full License](#)

It's all about the mirrors: Deep neural network assisted optimization of laser stabilization cavities

Johannes Dickmann^{1,+,*}, Liam Shelling Neto^{1,+}, Mika Gaedtke¹, and Stefanie Kroker¹

¹Technical University of Braunschweig, Institute for Semiconductor Technology, Hans-Sommer-Str. 66, 38106 Braunschweig, Germany

*j.dickmann@tu-braunschweig.de

⁺these authors contributed equally to this work

ABSTRACT

Ultra-stable laser cavities are the core components of today's most precise measurement instruments. To design and realize an ultra-stable laser cavity, one must suppress all kinds of noise below the desired frequency stability. The thermal noise of the cavity spacer sets a fundamental limit for the possible stability, especially for cavities operating at room temperature. We present a comprehensive numerical study of thermal cavity spacer noise, accounting for all relevant geometrical parameters. Accelerated by a vast amount of simulation data, a neural network is trained to predict spacer noise precisely for a wide range of all relevant cavity parameters. Based on this neural network, we identified design rules to reduce spacer noise by more than 50% by only changing the cavity geometry. Optimizing the cavity geometry and the material combination can achieve a noise reduction of more than two orders of magnitude without the infrastructural effort of a cryogenic environment.

Introduction

The use of ultra-stable lasers provides access to a wide range of phenomena in physics and applications in industry. For example, in optical atomic clocks, ultra-stable lasers are indispensable to address the narrow-linewidth electronic transitions^{1,2}. Also, interferometric gravitational wave detection is based on ultra-stable lasers^{3,4}. In industry, ultra-stable lasers are utilized for novel radar applications⁵ and deep space navigation⁶.

In general, all these ultra-stable lasers are stabilized using optical cavities, whereas different noise types limit the accessible frequency stability of these optical cavities. Thus, it is the general goal to reduce all limiting noise types resulting in a better stability, which would directly lead to better measurement sensitivity and the possibility of addressing new questions in physics.

The currently most stable laser systems are based on cryogenic mono-crystalline silicon spacers^{6,7}, reaching a frequency stability of 4×10^{-17} in terms of modified Allan deviation⁸. This stability is mainly limited by Brownian noise of the mirror

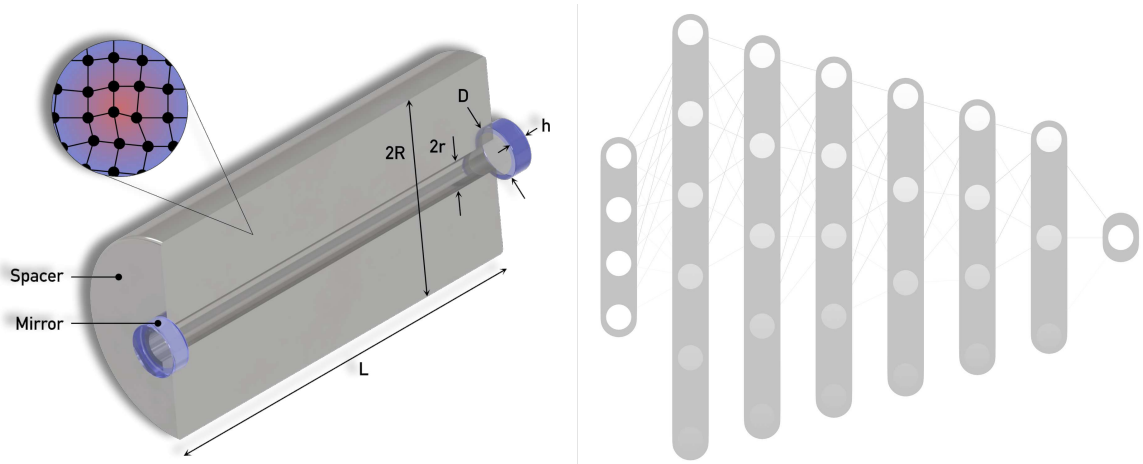


Figure 1. Laser cavity consisting of a spacer and two mirrors with highlighted geometrical parameters: The spacer length L , the spacer diameter $2R$, the bore diameter $2r$, as well as the mirror height h and the mirror diameter D . The spacer noise is illustrated as fluctuating atoms and the deep neural network for noise prediction beside.

coatings⁶. It is an enormous effort to implement and operate these systems in terms of infrastructure, time, and costs.

There are also ultra-stable lasers based on room-temperature optical cavities with only marginally worse frequency stability but associated with a significantly lower experimental effort. Specifically, these cavities reach frequency stabilities of 8×10^{-179} . For these room-temperature cavities, the frequency stability is mainly limited by Brownian noise of the cavity spacer⁹. Thus, there is a strong need for strategies to optimize cavity spacers to reach better stabilities even at room temperature.

In general, thermal noise can be computed utilizing the fluctuation-dissipation theorem¹⁰, which connects the thermal noise S and the elastic energy E under the force F :

$$S = \frac{4k_B T}{\pi f} \frac{E\phi}{F^2}, \quad (1)$$

where k_B is the Boltzmann constant, T the cavity temperature, f the measurement frequency and ϕ the mechanical loss, respectively. The most important consequence of the fluctuation-dissipation theorem for the design of optical cavities is that noise depends on both the geometry and the materials. In this work, we analyze for the first time, holistically, the influence of all geometrical parameters as well as all combinations of common materials for optical cavities on the frequency stability of the system. All geometrical parameters of the cavity are depicted in Fig. 1. The influences of the various parameters were investigated in large-scale simulation campaigns with over 18000 different parameter combinations. To handle the multitude and complex interplay of influences on the performance of the cavity, we implemented a deep neural network, which enables the optimization of the most important parameters for the lowest possible noise with great precision and speed.

Results

Evaluation of dominant cavity parameters

It is to be expected that not all parameters influence the noise equally. We computed a correlation matrix based on the vast number of simulations to clarify this. For that, we utilized the *pandas* Python package with Pearson correlation coefficients¹¹. The correlation matrix, shown in Fig. 2, visualizes the correlation of the geometrical cavity parameters as well as the Gaussian beam waist w and the elastic energy E , which is directly proportional to the spacer noise (compare Eq. (1)). Each combination of parameters is described by a correlation coefficient, where -1 and 1 correspond to perfect (anti-)correlation, and 0 exposes the lack of correlation of two parameters. Thus, by analyzing the correlation matrix, it becomes clear that further studies can disregard the influence of the bore radius r and the Gaussian beam waist w . The first essential and surprising result of this work is, that the mirror height h is by far the most critical parameter for spacer noise. The second most important parameter is the

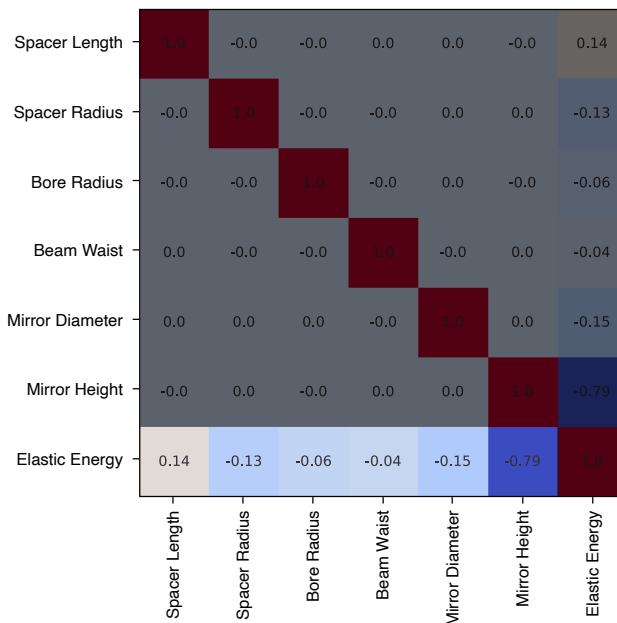


Figure 2. Correlation Matrix of all geometrical cavity parameters and the elastic energy, being proportional to the spacer noise. Most coefficients have been masked to improve readability.

mirror diameter. Therefore, the mirror dimensions are generally more important for spacer noise than the spacer dimensions themselves. Since the present work is the first analysis of the impact of the mirror dimensions on spacer noise, this strong result is a game-changer for the design of ultra-stable cavities.

Network optimization of critical cavity parameters

For the further procedure, we reduced the parameter space to be able to calculate more values of the dominant parameters, namely the mirror height h , the mirror diameter D , the spacer length L , and the outer spacer radius R . We trained a neural network to predict the elastic energy E for given geometrical parameters with a data set of 5248 different spacer geometries. The network was used to optimize the spacer geometry for minimized thermal noise by providing a vast number of data on the spot without the necessity of computationally expensive simulations. For the final design of the whole cavity setup, including vacuum chamber, temperature stabilization and vibration isolation⁹, the outer spacer radius R is the most critical one. Thus, this parameter was optimized first. For this purpose, the elastic energy was analyzed depending on the spacer radius. In Fig. 3 (a), the dependence of elastic energy and thus spacer noise is shown versus spacer radius for different spacer lengths L . The mirror height and diameter was set to 1 inch. The elastic energy decreases rapidly for increasing spacer radius. This result matches older studies on spacer noise^{12,13}. Apart from the thermal noise, also the vibration isolation benefits from a larger spacer radius^{14,15}. For both, vibration sensitivity and thermal noise, the benefit of increasing the spacer radius beyond a specific value is no longer worthwhile when manufacturing costs are taken into account. In Fig. 3 (a), the optimized spacer radius can be figured out for different spacer lengths. We defined an acceptable noise threshold to minimize the spacer radius and thus costs and infrastructural issues. This threshold was set to 10% of the ultimate noise limit at a maximum spacer radius of $R = 250$ mm. We obtained an optimized spacer radius for each spacer length and mirror size. The results of this analysis are depicted in Fig. 3 (b), depending on the spacer length and mirror size. We used mirrors with the same height as diameter in standard sizes. The mirror sizes range from 0.5 to 4 inches. For small mirrors up to 2 inches, the optimized spacer radius is proportional to the cavity length. For larger mirror substrates the dependency becomes nonlinear. In general, a larger mirror is also connected to a larger spacer radius for optimized thermal noise. In order to evaluate the benefit of the presented optimization compared to currently implemented spacer geometries, we will compare our results with an existing system in the following. To the best of our knowledge, the world's most stable laser cavity at room temperature is based on a 48 cm spacer consisting of ultra-low expansion glass (ULE)⁹. The frequency stability and thus the noise of this cavity is mainly limited by spacer noise⁹. This cavity consists of a spacer with a radius of 45 mm, a mirror diameter of 0.5 inches and a mirror height of about 6 mm⁹, resulting in a spacer noise of $S = 1.55 \times 10^{-34} \text{ m}^2/\text{Hz}$ at a frequency of 1 Hz. This noise equals a frequency stability limit of $\sigma = 2.5 \times 10^{-17}$ in terms of modified Allan deviation⁸. The best achievable frequency stability is depicted in Fig. 4 for different mirror sizes and is compared to the reference cavity. The stability is improved in the case of larger mirrors. The advantage is particularly noteworthy in the range of relatively small mirrors where current systems are operating. Compared to currently applied mirrors (dashed line in Fig. 4), the use of larger mirrors, for example, with a diameter of 2", would improve the stability by more than 50%.

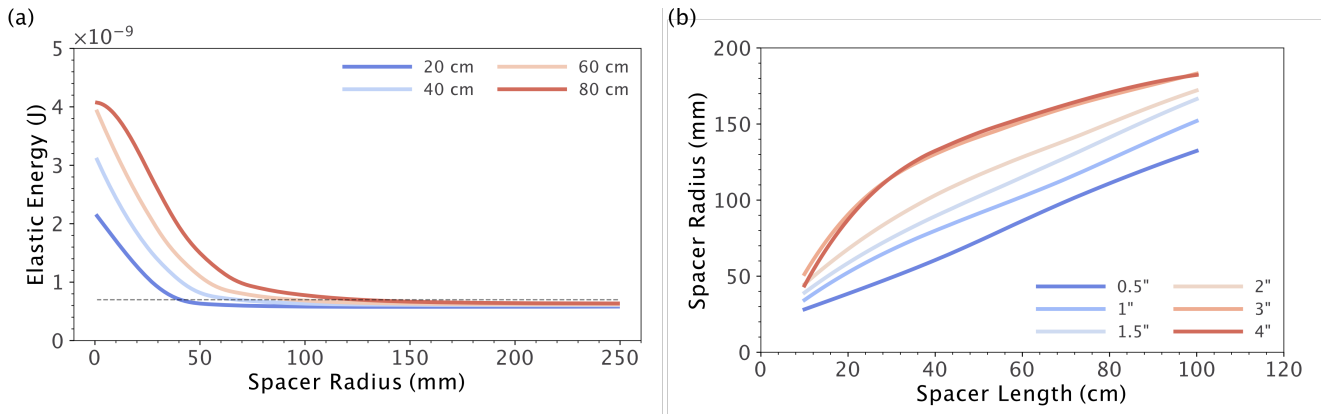


Figure 3. (a) Optimization of the spacer radius R : Elastic energy E versus spacer radius R for four exemplary different spacer lengths L . The energy approaches a minimum value at a certain spacer radius. The dashed line indicates the noise energy threshold set to 10% of the minimum value. (b) Results of the cavity radius optimization: The optimized spacer radius is shown versus cavity length for different mirrors between 0.5 inch and 4 inches.

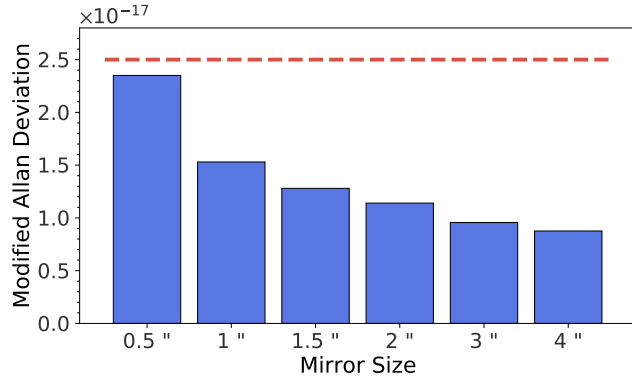


Figure 4. Best achievable frequency stability in terms of modified Allan Deviation limited by spacer noise for different mirror dimensions. The dashed line indicates the spacer noise of the currently most stable cavity operating at room temperature⁹.

Material Study

In addition to the spacer and mirror geometry, also the material combination influences spacer noise. For this reason, we have carried out a further analysis including all common material combinations for the spacer and mirror substrates. The materials are listed in Tab. 1, including all relevant material properties for the spacer noise. We performed a computation of spacer noise for the 48 cm cavity⁹ paired with 2" mirrors. We used the optimized values from the section above for the spacer radius. In this study, all possible material combinations for spacer and mirrors are analyzed. The common materials for spacers and mirror substrates are silicon⁷, fused silica¹⁶, ultra-low expansion glass (ULE)⁶, sapphire¹⁷ and diamond¹⁸. The material parameters necessary for noise calculation are listed in Tab. 1. The resulting spacer noise for all possible material combinations is shown in Fig. 5 in terms of best reachable modified Allan deviation limited by spacer noise. The currently used combination of ULE spacer and fused silica mirrors turns out to be one of the worst in terms of spacer noise. However, we see the discussed noise reduction of more than 50% due to optimized spacer and mirror geometry. It is possible to further decrease the spacer noise by one order of magnitude by using silicon as spacer material. Not surprisingly, the mirror material barely influences spacer noise. The use of silicon spacers reduces the spacer noise to achievable frequency stabilities of 2×10^{-19} , bringing room-temperature

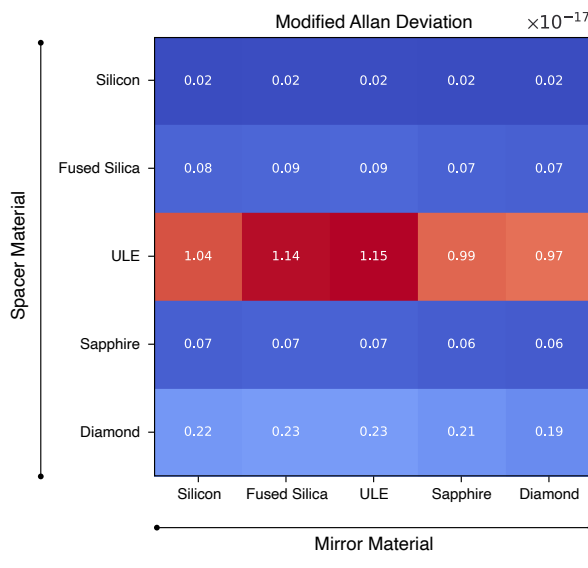


Figure 5. Material study on spacer noise: Modified Allan Deviation limit by spacer noise for different combinations of spacer and mirror material. All values are given for a 48 cm-long cavity with optimized spacer radius and 2" mirrors.

Material	Y (GPa)	σ (1)	ρ (kg/m ³)	ϕ 1
Silicon	165 ¹⁹	0.22 ¹⁹	2330 ¹⁹	1×10^{-8} ²⁰
Fused Silica	73 ²¹	0.16 ²¹	2201 ¹⁹	1×10^{-7} ²²
ULE	67.6 ²³	0.17 ²³	2210 ²³	1×10^{-7} ²³
Sapphire	463 ²⁴	0.309 ²⁴	3980 ²⁵	2.2×10^{-7} ²⁶
Diamond	1050 ²⁷	0.1 ²⁷	3515 ²⁸	6.7×10^{-6} ²⁹

Table 1. Properties of the most common materials for cavity spacer and mirrors at room temperature.

laser cavities to cryogenic performance.

Discussion

We have performed the first, to the best of our knowledge, universal analysis of thermal noise in spacers of optical cavities and presented it here. This answers many open questions in the current literature, especially the discrepancies of theoretical models^{12,13}. We identified the most critical parameters for spacer noise: Surprisingly, the mirror geometry is more important than the geometry of the spacer. In particular, the thickness of the mirror turned out to be the most crucial parameter. The next important parameter is the spacer radius. Since this parameter mainly affects the infrastructural requirement of the cavity, it was also minimized for minimal spacer noise. This analysis was performed for different mirror geometries. We implemented a deep neural network that predicts spacer noise precisely and fast, including all critical geometrical parameters. We compared the optimization results to the currently most stable laser cavity at room temperature. A noise reduction of more than 50 % could be achieved by just changing the mirror size and increasing the spacer radius. There are several common materials used to fabricate spacers and mirrors. We conducted a material study to rank the benefits of the different materials. It turned out that the mirror material has almost no influence on the spacer noise. In contrast, using silicon instead of ultra-low expansion glass would reduce the spacer noise by more than one order of magnitude. This would make room temperature cavities competitive with cryogenic ones while significantly reducing infrastructural effort.

Methods

Finite-Element Computation of Spacer Noise

The computation of spacer noise was carried out employing finite-element method using COMSOL Multiphysics³⁰. For the computation of thermal noise, we utilized the fluctuation-dissipation theorem (compare Eq. 1). In COMSOL, we evaluated the normalized elastic strain energy E/F^2 . All other quantities are either environmental parameters, universal or material constants. We implemented a two-dimensional COMSOL model in cylindrical coordinates to assess the normalized energy. For this purpose, the structural mechanics module was used with a stationary study. In the area of radiation pressure on the mirror, the mesh was manually refined. We utilized the parametric sweep feature of COMSOL to automatically compute spacer noise for more than 20000 cavities.

Neural Network for Spacer Noise

A parameter sweep that covers four parameters with appropriately small step sizes takes much time, considering the computational scope of one simulation carried out by finite-element method. As a much more efficient alternative, we utilized a data-driven deep neural network that is based on a relatively small amount of simulated samples. That way, we are able to decrease the time for obtaining the elastic energy for one parameter combination by a factor of 36 from 2 s to only 55 ms. The 5248 samples were separated into a training, validation and test set of 72 %, 18 % and 10 %, respectively. The network architecture consists of six fully connected layers where the number of neurons is halved with each subsequent layer, starting at 1024. Each layer uses the Leaky ReLU activation function ($\alpha = 0.3$) with a sigmoid activation in the regression layer. As an optimizer, we chose Adam³¹ with a learning rate of 0.001 and a decay value of 0.005. After 500 epochs, the network reached a MSE error of 2.15×10^{-6} and a R²-score of 0.99991 on the test set. Not only was the network able to understand the underlying information from the dataset to predict the elastic energy for every parameter combination within the borders of the simulated data. We observe an excellent agreement (deviation of less than 5 %) with parameter combinations outside of the dataset, i.e., extrapolation tasks. This unexpected behaviour could be an indicator that the network found a way to approximate an analytical, yet unknown, formula.

Data availability

The datasets generated during and/or analysed during the current study are available from the corresponding author on reasonable request.

References

1. Ludlow, A. D. Sr Lattice Clock at 1E-16 Fractional Uncertainty by Remote Optical Evaluation with a Ca Clock. *Science* **319**, 1802–1805, DOI: [10.1126/science.1153465](https://doi.org/10.1126/science.1153465) (2008).
2. Tamm, C., Weyers, S., Lipphardt, B. & Peik, E. Stray-field-induced quadrupole shift and absolute frequency of the 688-THz γ 171 b+ single-ion optical frequency standard. *Phys. Rev. A - At. Mol. Opt. Phys.* **80**, DOI: [10.1103/PhysRevA.80.043403](https://doi.org/10.1103/PhysRevA.80.043403) (2009).

3. Harry, G. M. *et al.* Thermal noise from optical coatings in gravitational wave detectors. *Tech. Rep.* (2006).
4. Abbott, B. P. *et al.* LIGO: The laser interferometer gravitational-wave observatory. *Reports on Prog. Phys.* **72**, DOI: [10.1088/0034-4885/72/7/076901](https://doi.org/10.1088/0034-4885/72/7/076901) (2009).
5. Ghelfi, P. *et al.* A fully photonics-based coherent radar system. *Nature* **507**, 341–345, DOI: [10.1038/nature13078](https://doi.org/10.1038/nature13078) (2014).
6. Matei, D. G. *et al.* $1.5\ \mu\text{m}$ Lasers with Sub-10 mHz Linewidth. *Phys. Rev. Lett.* **118**, DOI: [10.1103/PhysRevLett.118.263202](https://doi.org/10.1103/PhysRevLett.118.263202) (2017).
7. Kessler, T. *et al.* A sub-40-mHz-linewidth laser based on a silicon single-crystal optical cavity. *Nat. Photonics* **6**, 687–692, DOI: [10.1038/nphoton.2012.217](https://doi.org/10.1038/nphoton.2012.217) (2012).
8. Dawkins, S. T., McFerran, J. J. & Luiten, A. N. Considerations on the measurement of the stability of oscillators with frequency counters. *IEEE Transactions on Ultrason. Ferroelectr. Freq. Control.* **54**, 918–925, DOI: [10.1109/TUFFC.2007.337](https://doi.org/10.1109/TUFFC.2007.337) (2007).
9. Häfner, S. *et al.* 8E-17 fractional laser frequency instability with a long room-temperature cavity. *Opt. Lett.* **40**, 2112, DOI: [10.1364/ol.40.002112](https://doi.org/10.1364/ol.40.002112) (2015).
10. Levin, Y. Internal thermal noise in the LIGO test masses: A direct approach. *Phys. Rev. D* **57**, 659 (1998).
11. The pandas development team. *pandas-dev/pandas: Pandas* (2020).
12. Kessler, T., Legero, T. & Sterr, U. Thermal noise in optical cavities revisited. *J. Opt. Soc. Am. B* **29**, 178–184 (2012).
13. Numata, K., Kemery, A. & Camp, J. Thermal-noise limit in the frequency stabilization of lasers with rigid cavities. *Phys. Rev. Lett.* **93**, DOI: [10.1103/PhysRevLett.93.250602](https://doi.org/10.1103/PhysRevLett.93.250602) (2004).
14. Webster, S. A., Oxborrow, M. & Gill, P. Vibration insensitive optical cavity. *Phys. Rev. A - At. Mol. Opt. Phys.* **75**, DOI: [10.1103/PhysRevA.75.011801](https://doi.org/10.1103/PhysRevA.75.011801) (2007).
15. Webster, S. A., Oxborrow, M., Pugla, S., Millo, J. & Gill, P. Thermal-noise-limited optical cavity. *Phys. Rev. A - At. Mol. Opt. Phys.* **77**, DOI: [10.1103/PhysRevA.77.033847](https://doi.org/10.1103/PhysRevA.77.033847) (2008).
16. Legero, T., Kessler, T. & Sterr, U. Tuning the thermal expansion properties of optical reference cavities with fused silica mirrors. *J. Opt. Soc. Am. B* **27**, 914–919 (2010).
17. Taylor, C. T., Notcutt, M. & Blair, D. G. Cryogenic, all-sapphire, Fabry-Perot optical frequency reference. *Rev. Sci. Instruments* **66**, 955–960, DOI: [10.1063/1.1145629](https://doi.org/10.1063/1.1145629) (1995).
18. Janitz, E., Bhaskar, M. K. & Childress, L. Cavity quantum electrodynamics with color centers in diamond. *Optica* **7**, 1232, DOI: [10.1364/optica.398628](https://doi.org/10.1364/optica.398628) (2020).
19. McSkimin, H. J. Measurement of elastic constants at low temperatures by means of ultrasonic waves-data for silicon and germanium single crystals, and for fused silica. *J. Appl. Phys.* **24**, 988–997, DOI: [10.1063/1.1721449](https://doi.org/10.1063/1.1721449) (1953).
20. McGuigan, D. F. *et al.* Measurements of the Mechanical Q of Single-Crystal Silicon at Low Temperatures*. *Tech. Rep.* 5 (1978).
21. Musikant, S. *Optical materials: an introduction to selection and application*. (CRC Press, 2020).
22. Numata, K. *et al.* Measurement of the mechanical loss of crystalline samples using a nodal support. *Tech. Rep.* (2001).
23. Corning. *Corning Ultra-Low Expansion (ULE®) Glass* (2022).
24. Bernstein, B. T. Elastic constants of synthetic sapphire at 27°C. *J. Appl. Phys.* **34**, 169–172, DOI: [10.1063/1.1729059](https://doi.org/10.1063/1.1729059) (1963).
25. Tefft, W. E. Elastic constants of synthetic single crystal corundum. *J. Res. Natl. Bureau Standards. Sect. A, Phys. Chem.* **70**, 277 (1966).
26. Uchiyama, T. *et al.* Mechanical quality factor of a cryogenic sapphire test mass for gravitational wave detectors. *Tech. Rep.* (1999).
27. Güler, E. & Güler, M. Elastic and mechanical properties of cubic diamond under pressure. *Chin. J. Phys.* **53**, DOI: [10.6122/CJP.20141230](https://doi.org/10.6122/CJP.20141230) (2015).
28. Spear, K. E. & Dismukes, J. P. *Synthetic diamond: emerging CVD science and technology*. (John Wiley & Sons, 1994).
29. Tao, Y., Boss, J. M., Moores, B. A. & Degen, C. L. Single-crystal diamond nanomechanical resonators with quality factors exceeding one million. *Nat. Commun.* **5**, DOI: [10.1038/ncomms4638](https://doi.org/10.1038/ncomms4638) (2014).
30. COMSOL. *COMSOL Multiphysics® v. 6.0*.
31. Kingma, D. P. & Ba, J. Adam: A method for stochastic optimization. *arXiv* **1412** (2014).

Acknowledgements

Funded by the Deutsche Forschungsgemeinschaft (DFG, German Research Foundation) under Germany's Excellence Strategy – EXC-2123 QuantumFrontiers – 390837967

Author contributions statement

J.D. conceived the simulations and wrote the manuscript, L.S.N. analyzed the results and wrote the manuscript, M.G. and S.K. conceived the simulations. All authors reviewed the manuscript.

Competing interests

The authors declare no competing interests.